Neuron, Vol. 47, 515–528, August 18, 2005, Copyright ©2005 by Elsevier Inc. DOI 10.1016/j.neuron.2005.06.029

Regulation of EphA4 Kinase Activity Is Required for a Subset of Axon Guidance Decisions Suggesting a Key Role for Receptor Clustering in Eph Function

Joaquim Egea,[1] Ulla Vig Nissen,[2] Audrey Dufour,[3] Mustafa Sahin,[4] Paul Greer,[4] Klas Kullander,[5] Thomas D. Mrsic-Flogel,[1] Michael E. Greenberg,[4] Ole Kiehn,[2] Pierre Vanderhaeghen,[3] and Rüdiger Klein[1,*]

[1]Max-Planck Institute of Neurobiology
82152 Martinsried
Germany
[2]Department of Neuroscience
Karolinska Institute
17177 Stockholm
Sweden
[3]Institut de Recherches Interdisciplinaires en Biologie Humaine et Moléculaire (IRIBHM)
University of Brussels
Campus Erasme
B-1070 Brussels
Belgium
[4]Department of Neurology
Harvard Medical School
Children's Hospital
Boston, Massachusetts 02115
[5]Department of Neuroscience
Uppsala University
75124 Uppsala
Sweden

Summary

Signaling by receptor tyrosine kinases (RTKs) is mediated by their intrinsic kinase activity. Typically, kinase-activating mutations result in ligand-independent signaling and gain-of-function phenotypes. Like other RTKs, Ephs require kinase activity to signal, but signaling by Ephs in vitro also requires clustering by their membrane bound ephrin ligands. The relative importance of Eph kinase activity and clustering for in vivo functions is unknown. We find that knockin mice expressing a mutant form of EphA4 (EphA4^{EE}), whose kinase is constitutively activated in the absence of ephrinB ligands, are deficient in the development of thalamocortical projections and some aspects of central pattern generator rhythmicity. Surprisingly, other functions of EphA4 were regulated normally by EphA4^{EE}, including midline axon guidance, hindlimb locomotion, in vitro growth cone collapse, and phosphorylation of ephexin1. These results suggest that signaling of Eph RTKs follows a multistep process of induced kinase activity and higher-order clustering different from RTKs responding to soluble ligands.

Introduction

Guidance of navigating axons is mediated by long-range and short-range signals from surrounding cells. Short-range signals include cell or matrix-associated molecules, such as cell adhesion molecules and ephrins (Palmer and Klein, 2003). Ephrins are repulsive guidance cues at intermediate choice points, e.g., at the nervous system midline (reviewed in Kaprielian et al., 2001; Kullander and Klein, 2002) and for topographic mapping (reviewed in Vanderhaeghen and Polleux, 2004). Ephrins come in two flavors, GPI-anchored ephrinAs (A1–A5) and transmembrane ephrinBs (B1–B3). They bind and activate Eph receptors, the largest subfamily of receptor tyrosine kinases (RTKs), in a mostly subgroup-specific manner, i.e., A-type Ephs (EphA1–EphA8 and EphA10) bind ephrinAs, and B-type Ephs (EphB1–EphB4 and EphB6) bind ephrinBs, with few exceptions (Himanen et al., 2004). Because ephrins are connected to the plasma membrane, signaling can originate from the ephrin ligands as well as from the Eph receptors (reviewed in Kullander and Klein, 2002).

While the mechanisms by which Ephs and ephrins regulate diverse biological functions are beginning to be understood, our knowledge about the regulation of Eph receptor activation and downstream signaling is rather incomplete. Eph receptors resemble in many respects classical RTKs (Schlessinger, 2000): they show ligand-induced autophosphorylation and kinase activation, they recruit adaptor proteins, and most if not all in vivo functions mediated by Eph signaling require an intact kinase activity (Kullander et al., 2001b). Like several other RTKs, they are kept in an autoinhibited state by their juxtamembrane (JM) region (Gille et al., 2000; Herbst and Burden, 2000; Wybenga-Groot et al., 2001). The unphosphorylated JM region interacts intramolecularly with the kinase domain and forces it into an inactive conformation (Wybenga-Groot et al., 2001). Phosphorylation of specific tyrosine residues within the JM region relieves autoinhibition.

Unlike other RTKs, Eph receptors are activated exclusively by membrane bound ligands but not by soluble monomeric ligands (Davis et al., 1994). When expressed as soluble dimers fused to the Fc portion of human IgG, ephrins have weak activation potential (Davis et al., 1994; Stein et al., 1998) and in vivo can act as dominant-interfering ligands (Gerlai et al., 1999). When aggregated in solution or bound to beads, ephrins trigger the formation of Eph clusters (Wimmer-Kleikamp et al., 2004) and elicit full Eph signaling (Davis et al., 1994; Stein et al., 1998). These data suggest that Ephs are activated by two processes: kinase activation and higher-order clustering. The relative importance of these events is not understood. Moreover, the importance of Eph-ephrin clustering for the diverse biological functions in vivo is unclear and has so far not been addressed genetically. Previous work has shown that clustered Ephs recruited the effector low-molecular weight phosphotyrosine phosphatase (LMW-PTP) (Stein et al., 1998). The significance of recruitment of LMW-PTP for normal Eph function is, however, unclear (Chiarugi et al., 2004).

Here, we have addressed the relative importance of kinase activity and clustering for several developmental

*Correspondence: rklein@neuro.mpg.de

functions of the EphA4 receptor. First, EphA4 has a non-cell-autonomous role, not requiring EphA4 forward signaling in the formation of the anterior commissure (AC), an axon bundle that connects the two cerebral hemispheres (Cowan et al., 2004; Kullander et al., 2001b). Second, EphA4 is required for development of the thalamocortical system, where complementary gradients of EphA4 in the thalamic primary somatosensory (ventrobasal [VB]) nucleus, and ephrinA5 in the somatosensory area (S1) of the cortex, control topographic mapping of thalamocortical axons (Dufour et al., 2003). Third, EphA4 is required for corticospinal tract (CST) axons to recognize the spinal cord midline as an intermediate repulsive target that prevents them from aberrantly recrossing (Kullander et al., 2001a, 2001b; Yokoyama et al., 2001). Fourth, EphA4-positive neurons are key components of the spinal central pattern generator (CPG) (Kullander et al., 2003; reviewed in Kiehn and Kullander, 2004), a local neuronal network within the spinal cord that is rhythmically active during locomotion (Butt and Kiehn, 2003; Kiehn and Kjaerulff, 1998).

Kinase activation is the critical and regulated step for most RTKs (Schlessinger, 2000). The biological activity of most RTKs strictly correlates with the degree of enzymatic activation. Mutations that result in constitutive receptor activation are frequently observed in cancer, and ectopic expression of constitutively active RTK mutants generally causes gain-of-function phenotypes, such as hyperproliferation or cell transformation (Holland et al., 1998; Sommer et al., 2003). Based on structural information and previous work on the related EphB2 receptor (Wybenga-Groot et al., 2001; Zisch et al., 2000), we generated an EphA4 receptor carrying a constitutively activated kinase by replacing two JM tyrosine residues with glutamate residues (termed kinase-active EphA4^{EE}). Here, we show that mice expressing kinase-active EphA4^{EE} were deficient in the development of thalamocortical projections and some aspects of CPG rhythmicity. Surprisingly, other functions of EphA4 were regulated normally by EphA4^{EE}, including midline guidance of CST and CPG axons. These results indicate that EphA4 kinase activity, although required, is not sufficient for EphA4 forward signaling in vivo. In vitro, clustering of kinase-active EphA4^{EE} induced normal growth cone collapse and phosphorylation of the downstream effector ephexin1, suggesting that Eph signaling output and cellular responses are regulated by induction of kinase activity and higher-order clustering.

Results

Generation of a Constitutively Active EphA4 Receptor

Structural information on EphA4 and the related EphB2 cytoplasmic domains (Wybenga-Groot et al., 2001) pointed to two tyrosines (Y596 and Y602) of the EphA4 JM region, which in the unphosphorylated form associate with the Eph kinase domain and autoinhibit the receptor. Phosphorylation of these tyrosine residues, or replacement by glutamic acid, relieved autoinhibition without negatively affecting forward signaling (Wybenga-Groot et al., 2001; Zisch et al., 2000). To extend these observations, we engineered the Y596E/Y602E mutant in EphA4 (here referred to as EphA4^{EE}; Figure 1A) and characterized its kinase activity toward a newly designed in vitro substrate of EphA4: its own JM domain fused to glutathione S-transferase (GST-JM; see Experimental Procedures). Immunoprecipitated EphA4 from EphA4-transfected HEK293 cells was able to phosphorylate the GST-JM substrate but not GST alone (see Figure S1A in the Supplemental Data available with this article online). Phosphorylation of GST-JM was reliably observed in the presence of wild-type EphA4 and mutant EphA4^{EE}, but not kinase-dead EphA4 (Figure S1B). To investigate if the regulation of EphA4 kinase activity is required for axon pathfinding in vivo, we generated mice in which the wild-type *ephA4* gene was replaced by a mutant version of *ephA4* encoding the EphA4^{EE} receptor. We used the same knockin strategy as for kinase-dead EphA4 (*ephA4^{KD}* allele; Kullander et al., 2001b) and C-terminally truncated EphA4 (*ephA4^{GFP}* allele; Grunwald et al., 2004) (Figures 1A–1C). The expression levels of EphA4 protein in embryonic brain lysates derived from *ephA4$^{EE/EE}$* mutant mice were similar to those of wild-type (+/+) littermates or wild-type *ephA4* knockin control animals (*ephA4$^{WT/WT}$*; Figure 1D; and data not shown). The EphA4^{EE} protein displayed somewhat slower mobility in SDS-PAGE, possibly due to the additional negative charge provided by the two glutamic acids (Figure 1D).

To evaluate the activity of the EphA4^{EE} protein expressed by the targeted *ephA4* locus, we derived primary cortical neurons from embryonic day 16.5 (E16.5) *ephA4$^{EE/EE}$* mutant embryos and assayed its in vitro kinase activity toward the GST-JM substrate. Basal EphA4 kinase activity in *ephA4$^{EE/EE}$* neurons was increased approximately 3.5-fold compared to *ephA4$^{WT/WT}$* neurons (Figure 1E). This is in agreement with the reported increase of kinase activity in other RTK mutants (Bardelli et al., 1998; Chen et al., 1997; Pasini et al., 1997). The increased kinase activity of EphA4^{EE} could not be further enhanced by stimulation with ephrinB3-Fc (Figure 1F, right). In contrast, stimulation of *ephA4$^{WT/WT}$* neurons for 20 and 40 min caused a 2-fold induction of kinase activity above nontreated or control Fc-treated levels (Figure 1F, left). EphA4^{EE} receptor autophosphorylation was greatly reduced compared to wild-type EphA4, confirming that the two JM tyrosine residues were the major sites of autophosphorylation. Prolonged stimulation with ephrinB3-Fc slightly increased EphA4^{EE} tyrosine phosphorylation, consistent with observed autophosphorylation of tyrosine residues in the activation loop (Wybenga-Groot et al., 2001) (Figure S1C). To exclude that EphA4 kinase activity was activated by clustering during the immunoprecipitation, we measured EphA4 kinase activity after eluting it from the immunoprecipitating antibodies. Under these conditions, we still observed a ligand-dependent 2-fold increase in kinase activity of wild-type EphA4. In contrast, the higher basal kinase activity of EphA4^{EE} was not further enhanced by stimulation with ephrinB3-Fc (Figure 1G; Figure S1D). Finally, we attempted to measure EphA4 kinase activity toward the GST-JM substrate in living

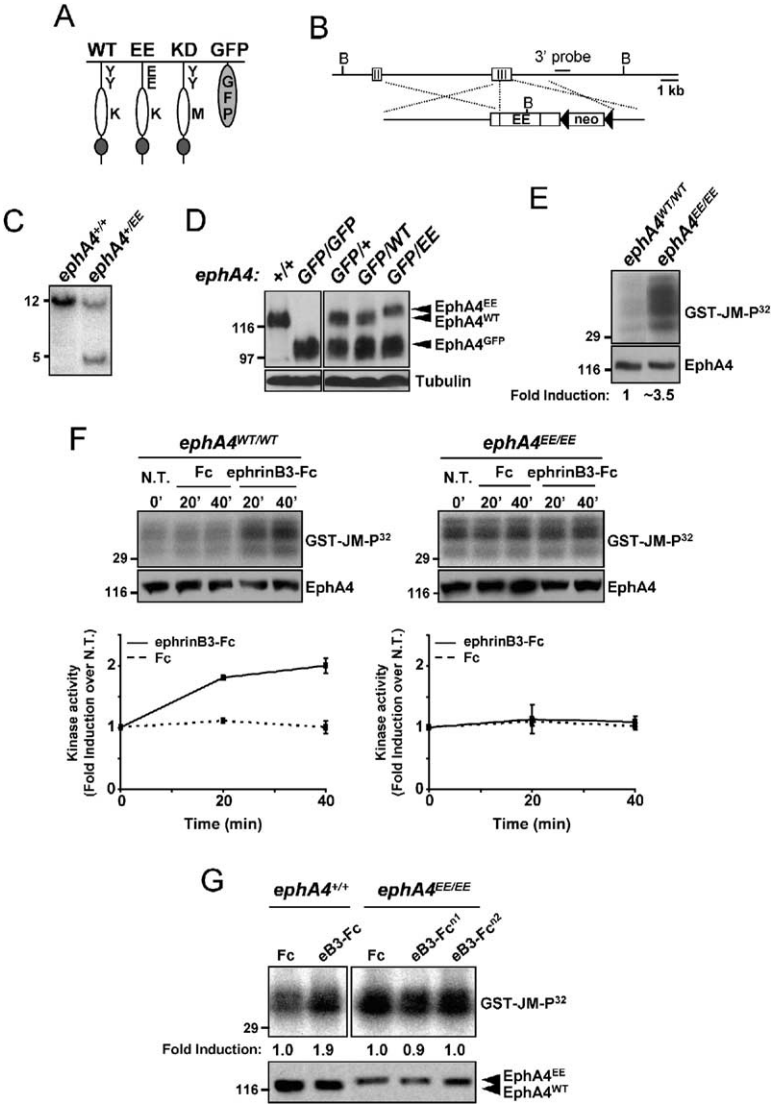

Figure 1. Generation of a Knockin Mouse Expressing a Constitutively Active EphA4 Receptor

(A) Schematic models of the intracellular part of the EphA4 receptor encoded by different *ephA4* mutant alleles used in the present study. WT, wild-type control allele of the targeting strategy; EE, mutant allele in which the two juxtamembrane tyrosines (Y596 and Y602) were replaced by two glutamic acid residues; KD, kinase-dead receptor in which lysine K653 in the catalytic domain and responsible for ATP binding was mutated to a methionine residue (M). GFP, mutant allele encoding an EphA4 receptor whose entire intracellular part was replaced by green fluorescent protein.

(B and C) Schematic representation of the homologous recombination strategy used to mutate the mouse *ephA4* gene. Replacement-type vector containing the $ephA4^{EE}$ cDNA (EE) was fused in frame with the third exon (III) and thereby placed under control of the endogenous gene promoter. A loxP-flanked (black triangles) neomycin selection marker was subsequently removed by the Cre recombinase. BamHI restriction sites (B) and location of the Southern hybridization probe are indicated. Southern hybridization with ES cell genomic DNA following enzymatic restriction by BamHI. The probe corresponding to intronic sequences adjacent to the 3′ end of the targeted region detected a 12.5 kb wild-type (+/+) and a 4.6 kb targeted DNA fragment in clones of transfected $ephA4^{EE}$ (EE/+) ES cells (C).

(D) Western blot analysis against EphA4 in extracts of embryonic brains (E16.5) from the indicated mutants. The $ephA4^{EE}$ and control alleles were tested in combination with the $ephA4^{GFP}$ allele, whose faster migration allowed the separation by size and provided an internal control. Expression levels of $EphA4^{EE}$ protein were comparable to those of endogenous EphA4 (+) and cDNA-encoded $EphA4^{WT}$ protein. Note the slightly slower mobility of the $EphA4^{EE}$ receptor compared to wild-type EphA4.

(E) EphA4 kinase activity toward the exogenous substrate GST-JM in immunoprecipitates from cortical neurons derived from control $ephA4^{WT/WT}$ or $ephA4^{EE/EE}$ neurons. Basal EphA4 kinase activity was 3.5-fold higher in $ephA4^{EE/EE}$ compared to $ephA4^{WT/WT}$ neurons (average of n = 3 experiments).

(F) EphA4 kinase activity in immunoprecipitates from cultured cortical neurons of $ephA4^{WT/WT}$ or $ephA4^{EE/EE}$ mice stimulated with preclustered ephrinB3-Fc or Fc control protein for the indicated time points. The experiments were otherwise done as in (E). In $ephA4^{WT/WT}$ neurons, ephrinB3 induced kinase activity 2-fold above Fc control stimulation (kinase activity before stimulation was set to 1). In $ephA4^{EE/EE}$ neurons, no significant increases above basal levels were measured at either 20 min or 40 min poststimulation (N.T., nontreated cultures) (average of n = 2 experiments). Data were expressed as the average ± SEM.

(G) EphA4 kinase activity of the nonclustered receptor after elution from the immunoprecipitating antibodies. EphrinB3 (eB3-Fc) stimulation and immunoprecipitations were done as in (E) and (F). The receptor was released from the beads using 30–40 μg of the KLH-coupled $EphA4^{C\text{-}term}$ peptide per sample as described in Figure S1D. In vitro kinase activity was carried out using GST-JM as exogenous substrate. The background activity obtained in sibling samples using protein A beads only (without antibody) or in EphA4 immunoprecipitates without adding exogenous substrate was subtracted from each kinase activity value. Activity was expressed as fold induction over Fc-treated samples. Lower panel shows the amount of EphA4 receptor in the original neuron lysates used for the kinase assay. Basal kinase activity of $EphA4^{EE}$ compared to wild-type EphA4 was increased 2.6-fold in the immunoprecipitates and 2.3-fold after elution.

cells. To this end, we coexpressed EphA4 together with GST-JM in HeLa cells, stimulated the cells with ephrinB3-Fc or control Fc, and measured the phosphorylation of GST-JM by pull-down with glutathione beads followed by anti-phosphotyrosine immunoblotting. Under these conditions, the in vivo phosphorylation of GST-JM was greatly enhanced in the presence of $EphA4^{EE}$ compared to wild-type EphA4 (Figure S2). In summary, these results indicate that the $EphA4^{EE}$ receptor displays greatly increased kinase activity and suggest that the mutant $ephA4^{EE}$ allele is a specific gain-of-function allele with respect to its tyrosine kinase activity.

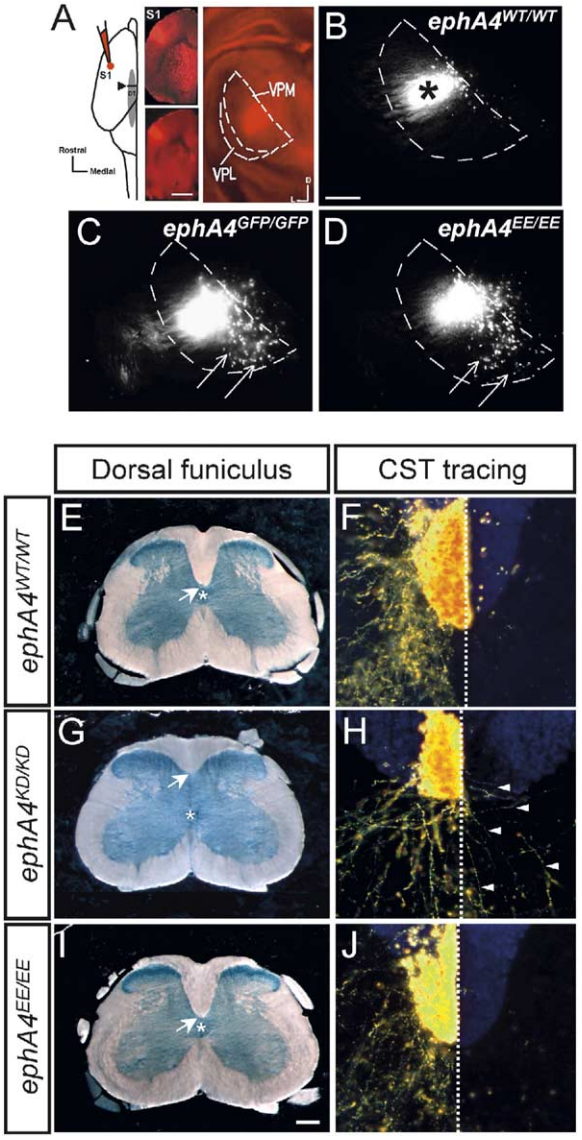

Figure 2. Abnormal Thalamocortical Projections but Normal Midline Behavior of Corticospinal Tract Fibers in *ephA4*$^{EE/EE}$ Mutant Mice

(A–D) The point-to-point topography of projections between the thalamic nucleus VB (subdivided into a medial and a lateral part: VPM and VPL, respectively) and the primary somatosensory area S1 demonstrated by retrograde labeling (schematic drawing and low-power views in [A]). (B) In control *ephA4*$^{WT/WT}$ mice, focal injection of DiI in S1 resulted in the retrograde labeling of a single cluster of cells in the thalamic nucleus VPM (asterisk). In contrast, the *ephA4*$^{GFP/GFP}$ and *ephA4*$^{EE/EE}$ mutants showed, in addition to the normal cluster, ectopic cells located more medially to their normal location (arrows), suggesting that thalamocortical projections were not properly organized in the mutants (C and D). Scale bars equal 1500 μm in (A) (small pictures) and 400 μm in (B). (E, G, and I) Dark-field photographs of spinal cord cross-sections at the thoracolumbar level of the indicated mutant mice showing the regular shape of the dorsal funiculus in *ephA4*$^{EE/EE}$ and *ephA4*$^{WT/WT}$ mice. Note the shorter ventral extension of the dorsal funiculus in the *ephA4*$^{KD/KD}$ mutant (longer distance between the ventral tip of the dorsal funiculus [arrow] and the central canal [asterisk]). Scale bar in (I) equals 250 μm. (F, H, and J) The motor cortex of anesthetized mice was traced unilaterally (right hemisphere) with biotin dextran amine, and mice were sacrificed 7–9 days afterwards. On vibratome sections, CST axons were only occasionally seen to recross the midline in the brachial part of the spinal cord in *ephA4*$^{WT/WT}$ and *ephA4*$^{EE/EE}$ mice. In contrast, many CST fibers (arrowheads in [H]) recrossed the midline in *ephA4*$^{KD/KD}$ mutants.

The Kinase-Active EphA4^{EE} Receptor Mediates Pathfinding Events Triggered by EphrinB Reverse Signaling

Since *ephA4*$^{EE/EE}$ mice were viable and fertile, we first asked whether kinase-active EphA4 would mediate AC formation. EphA4 is expressed by cells in the territory through which AC axons travel and induces ephrinB reverse signaling in AC axons (Cowan et al., 2004; Kullander et al., 2001b). EphA4 kinase activity is not required for this process (Kullander et al., 2001b). To visualize the AC, we analyzed horizontal forebrain sections of 12- to 16-week-old mice under bright-field microscopy. The anterior limb of the AC (aAC) appears as a horseshoe-shaped axon bundle, which colocalizes with the medial part of the posterior limb (pAC). Both portions were normally developed in control *ephA4*$^{WT/WT}$ and *ephA4*$^{EE/EE}$ mutant knockin mice (n = 4 mice), while in the majority of *ephA4*$^{null/null}$ mutants both limbs fail to cross the midline and misproject to aberrant target regions on the ipsilateral sides (Figure S3) (see also Kullander et al., 2001b). These results indicate that kinase-active EphA4^{EE} triggered normal ephrinB reverse signaling on AC axons, suggesting that the protein is properly located in the plasma membrane.

ephA4$^{EE/EE}$ Mutants Have Abnormal Thalamocortical Projections

We next analyzed the topographic projections of dorsal thalamic axons to the somatosensory cortex, which were shown to require the presence of EphA4 (Dufour et al., 2003). The area specificity and topography are controlled by ephrinA5, which is expressed in a low lateral to high medial gradient in S1, and by EphA4, which is expressed in a complementary gradient in the thalamic primary somatosensory nucleus (VB). In *ephA4*$^{WT/WT}$ (n = 6) animals, a single injection of the retrograde tracer DiI into the S1 barrel cortex systematically resulted in the labeling of a single cluster of cells in the ventro-postero-medial nucleus (VPM) of the somatosensory thalamus (Figures 2A and 2B) (see also Dufour et al., 2003). When similar injections had been performed in *ephA4*$^{null/null}$ animals, a significant proportion of the retrogradely labeled thalamic cells were located more medially than the normal cluster (penetrance 43%; n = 7 out of 16) (Dufour et al., 2003). *EphA4*$^{GFP/GFP}$ mutants showed the same phenotype as *ephA4*$^{null/null}$ animals, indicating that correct establishment of thalamocortical projections required EphA4 forward signaling (penetrance 83%; n = 5 out of 6) (Figure 2C, arrows). Interestingly, the *ephA4*$^{EE/EE}$ mutants phenocopied the forward signaling-deficient *ephA4*$^{GFP/GFP}$ mutants, indicating that the EphA4^{EE} receptor was not able to properly organize these projections (penetrance 61%; n = 8 out of 13) (Figure 2D, arrows). The expression levels of EphA4 in the thalamus of *ephA4*$^{EE/EE}$ mice were comparable to those of *ephA4*$^{WT/WT}$ mice (Figure S1E), indicating that the defect observed in the mutant mice could not be attributable to reduced expression of the

receptor in this particular area of the brain. These results rather suggest that regulation of kinase activity by ephrins is required for EphA4-mediated topographic mapping of thalamocortical somatosensory projections.

The *ephA4*^{EE} Allele Rescues the CST Phenotype of *ephA4* Loss-of-Function Alleles

CST axons originate in the motor cortex, traverse the midline at the brain-spinal cord junction, and then continue down in the opposite side of the spinal cord to ultimately connect with spinal cord motor neurons. The interaction between midline ephrinB3 and EphA4 on CST axons prevents these axons from aberrantly recrossing the spinal cord midline (Kullander et al., 2001a, 2001b; Yokoyama et al., 2001). We hypothesized that kinase-active EphA4^{EE} receptors would perhaps cause a gain-of-function phenotype resulting in ephrin-independent growth cone collapse and failure of axon tract formation. Constitutive activation of EphA4 kinase activity may have also increased EphA4 endocytosis and trafficking and may have reduced sensitivity toward ephrin-induced repulsion. To our surprise, however, *ephA4*$^{EE/EE}$ mice displayed normal CST projections. The *ephA4*$^{null/null}$ mutant CST phenotype has two components, which are likely to be linked. First, the dorsoventral extent of the dorsal funiculus is reduced, possibly due to loss of CST axons, and secondly, CST fibers within the dorsal funiculus aberrantly recross the midline at lumbar levels of the spinal cord (Kullander et al., 2001a, 2001b; Yokoyama et al., 2001). Histological analysis of spinal cord cross-sections of *ephA4*$^{null/null}$ and *ephA4*$^{KD/KD}$ mutants revealed the expected reductions of white matter in the dorsal funiculus in both the brachial (data not shown) and lumbar regions (compare Figures 2E and 2G; and data not shown). In contrast, the *ephA4*$^{EE/EE}$ mutants displayed a normal dorsal funiculus (n = 6 animals) (Figure 2I). To visualize CST axons, we performed unilateral, anterograde, axon-tracing experiments in the motor cortex and stained the terminal projections of the CST in the spinal cord. In *ephA4*$^{WT/WT}$ animals, stained CST axons project only to one side of the spinal cord, which is contralateral to the tracer injection side (Figure 2F). Aberrant recrossings through the midline into the ipsilateral side were rarely observed (three out of ten sections presented at least one aberrant axon). In contrast, in *ephA4*$^{KD/KD}$ spinal cords, 100% of the sections showed many aberrant axon sprouts that recrossed the midline (Figure 2H) (see also Kullander et al., 2001b). Interestingly, and consistent with the normal shape of the dorsal funiculus, the *ephA4*$^{EE/EE}$ mice had normal unilateral CST projections (Figure 2J), indicating that the kinase-active EphA4^{EE} receptor elicits normal forward signaling to mediate midline repulsion of CST axons.

The CPG Circuit Is Partially Abnormal in *ephA4*$^{EE/EE}$ Mice

Locomotion, though controlled from higher motor centers in the brain, is produced by neuronal networks within the spinal cord called central pattern generators (CPGs) and consists of stereotyped actions involving repetitions of the same movement. The lower thoracic and upper lumbar spinal cord is the region that is most rhythmically active during locomotion (Cowley and Schmidt, 1997; Kjaerulff and Kiehn, 1996; Kremer and Lev-Tov, 1997). EphA4-positive neurons are important components of the CPG (Kullander et al., 2003). In *ephA4* and *ephrinB3* null mutants, a significant fraction of these neurons aberrantly project contralaterally and cause reciprocal overexcitation of the CPG resulting in a hopping gait (Kullander et al., 2003). To investigate EphA4 kinase signaling in local spinal CPG development, we examined locomotor-like behavior in isolated spinal cord preparations from newborn mice (Figure 3A). In wild-type or heterozygous control mice, rhythmic locomotor activity induced by addition of serotonin (5-HT) and N-methyl-D-aspartic-acid (NMDA) was characterized by alternation between the left lumbar (L) segment 2 and right L2 ventral root bursts, similar to left-right alternation between hindlimbs (Kullander et al., 2003) (Figure 3B1). There was also alternation between L2 and L5 activity on the same side of the spinal cord, similar to the flexion and extension in one limb during locomotion. In contrast, bilateral roots of *ephA4*$^{null/null}$ mutants displayed abnormal synchronous rhythm (Figure 3B2; Kullander et al., 2003). The pattern in *ephA4*$^{EE/EE}$ mice was normal at the L2 level: 12 out of 14 preparations demonstrated significant alternation compared to eight out of nine control preparations (Figures 3B3, 3C1, and 3C4). At the L5 level, however, *ephA4*$^{EE/EE}$ mice gave mixed results: only one out of ten preparations showed alternation, six were drifting (see Experimental Procedures), and three showed synchrony compared to five out of eight control preparations showing significant alternation (Figures 3C3 and 3C6). The ipsilateral coupling between L2-L5 roots was only significant in half the *ephA4*$^{EE/EE}$ preparations (7 out of 13). This finding suggests looser coupling of the ipsilateral coordination in the *ephA4*$^{EE/EE}$ mice than in controls (Figures 3C2 and 3C5).

Normal left-right coordination is mediated by commissural interneurons (CINs), whose cell bodies are located in the ventral spinal cord. Tracing of CINs by midline staining and tracing of ascending or descending CINs in *ephA4*$^{EE/EE}$ mice showed no obvious deviation from normal mice or *ephA4*$^{null/null}$ mice at either the L2 or the L5 level (data not shown and Figures 3D–3F). Importantly, we did not observe in *ephA4*$^{EE/EE}$ mutants the increased aberrant crossing of descending fibers that we previously detected in *ephA4*$^{null/null}$ and *ephrinB3*$^{null/null}$ mice (Figures 3E and 3F; Kullander et al., 2003). These results indicate that the kinase-active EphA4^{EE} receptor is able to recognize the midline repellent ephrinB3, thus "avoiding" aberrant crossing in the spinal cord. The EphA4^{EE} receptor mediates the development of a semifunctional CPG that is normal with respect to the L2 coordination, but not the L5 and the ipsilateral L2-L5 coordination.

Normal Unilateral Motor Control in *ephA4*$^{EE/EE}$ Mice

An intact CPG circuit is essential for normal walking behavior. Mice either lacking EphA4 or expressing a kinase-dead mutant of EphA4 move their hindlimbs synchronously in a hopping fashion. Because *ephA4*$^{EE/EE}$ mice displayed abnormal locomotor patterns in iso-

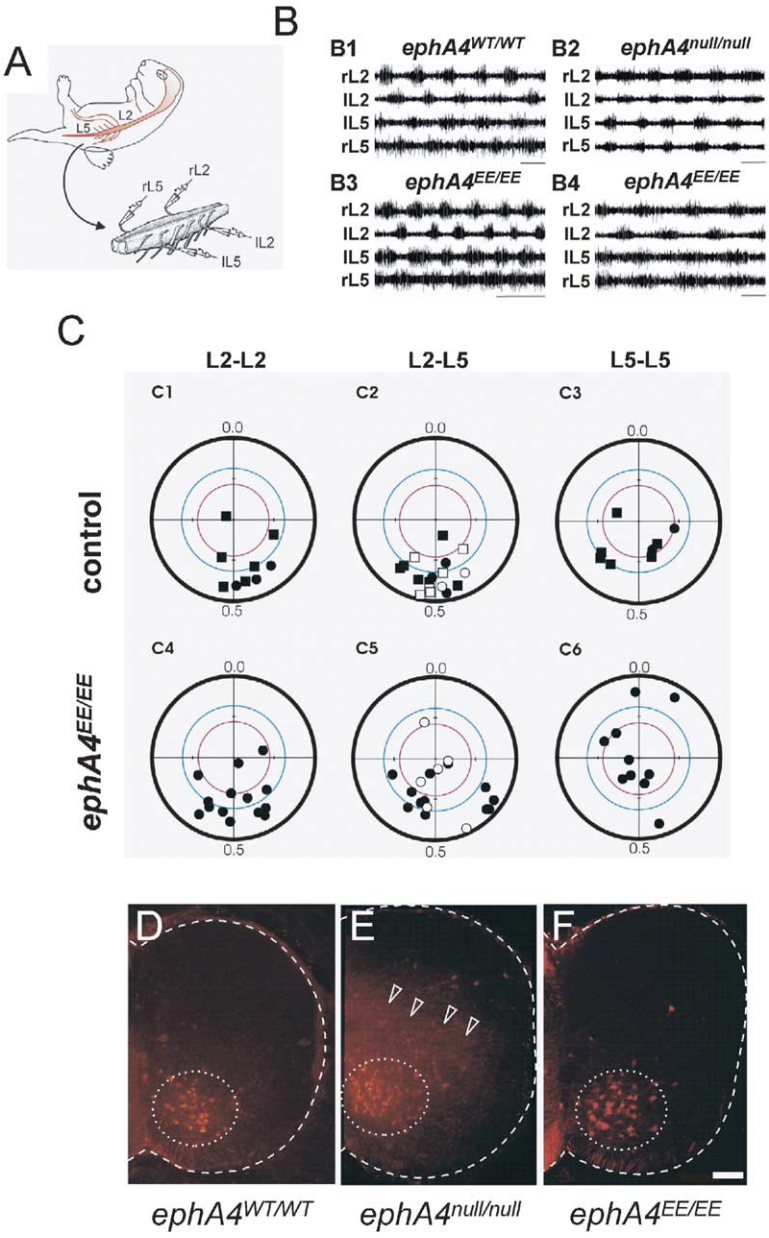

Figure 3. Partially Abnormal Left-Right Synchrony and Normal Midline Axon Pathfinding in *ephA4*$^{EE/EE}$ Spinal Cords

(A) Experimental setup to record fictive locomotion in the in vitro mouse spinal cord preparation. Suction electrodes were placed on both the right and left ventral roots at lumbar levels 2 and 5. Fictive locomotion was induced by perfusion with a combination of NMDA and serotonin (5-HT).

(B1–B4) Recordings of locomotor activity in an *ephA4*$^{WT/WT}$ mouse (B1), a homozygous *ephA4*$^{null/null}$ mouse (B2), and two *ephA4*$^{EE/EE}$ mice (B3 and B4). Note alternation between left (l) and right (r) L2 in control and the two *ephA4*$^{EE/EE}$ mice. Synchrony is observed in *ephA4*$^{null/null}$ mutants. At L5 level, one of the *ephA4*$^{EE/EE}$ mice alternates (B3), while the other displays synchrony (B4). Timescale equals 1 s.

(C1–C6) Circular phase diagrams showing the significance level of the locomotor pattern. Blue circles indicate high significance ($p < 0.001$; dots outside the blue line), red circles indicate significance ($0.05 < p < 0.001$; dots outside the red line), and dots inside the red line are nonsignificant (NS). (C1) Control group at L2 level consisting of three wild-type (dots) and six heterozygotes (squares). Eight out of nine preparations show significant alternation. (C4) In *ephA4*$^{EE/EE}$ mice at L2 level, locomotion is normal in 12 out of 14 preparations. (C2 and C5) Ipsilateral coupling between the left L2/L5 roots (black dots) and right L2/L5 roots (white dots). (C2) Locomotion is normal in the control group, with only one out of nine preparations being nonsignificant. (C5) Locomotion is seminormal in *ephA4*$^{EE/EE}$ mice, with only 7 out of 13 preparations showing significant alternation. (C3 and C6) Coupling between the two L5 roots. (C3) Locomotion is near normal in the control group, with five out of eight preparations showing significant alternation. (C6) Locomotion is abnormal in *ephA4*$^{EE/EE}$ mice, with most of the preparations either being nonsignificant or showing synchrony.

(D–F) Tracing of descending commissural interneurons (dCINs) at L2 level. Transverse spinal cord sections showing the distribution of dCINs after application of RDA between the L3/L4 root. No overt difference is observed in the distribution of dCINs in control (D), *ephA4*$^{null/null}$ (E), and *ephA4*$^{EE/EE}$ mice (F) (white dotted line). However, fibers extensively cross the midline in *ephA4*$^{null/null}$ mutants ([E]; arrowheads), but not in wild-type (D) or *ephA4*$^{EE/EE}$ mice (F). The preparation in (F) was traced after recording, where it showed synchrony in L5 roots and therefore represents the most abnormal *ephA4*$^{EE/EE}$ case. Scale bar, 100 μm.

lated spinal cord preparations, we subjected adult animals to a gait analysis (Kullander et al., 2001a). Visual inspection of the footprints of *ephA4*$^{WT/WT}$ control and *ephA4*$^{EE/EE}$ mice revealed a normal alternating step pattern with the placement of each hindpaw where the forepaw had been (Figure 4A). In contrast, mice expressing signaling-deficient EphA4^{GFP} receptors moved by first hopping on their two front paws and then hopping on their two hindpaws (Figure 4A). To minimize differences in sex, body weight, or speed of locomotion, we calculated the ratio between the distances covered by left and right paw (B) and the distance covered by the same paw (A) (Figure 4B). During perfect alternation, the ratio B/A approximates the value 0.5. During parallel hopping, the ratio B/A approximates the value 0.0. When applying this ratio to *ephA4*$^{EE/EE}$ animals and to *ephA4*$^{WT/WT}$ littermate controls from two independent breedings, we could not detect any significant differences between both groups of mice (Figure 4C). Neither could we detect differences when we included one copy of the inactive *ephA4*^{GFP} allele to sensitize the phenotype (Figure 4D). Only *ephA4*$^{GFP/GFP}$ or *ephA4*$^{KD/KD}$ mutant mice displayed synchronicity of the hindlimbs resulting in a ratio B/A close to zero (Figure 4E). These results show that adult *ephA4*$^{EE/EE}$ mutant mice have normal gait as evaluated by footprint analysis, indicating that in the presence of an intact sensory feedback loop paw placement is normal.

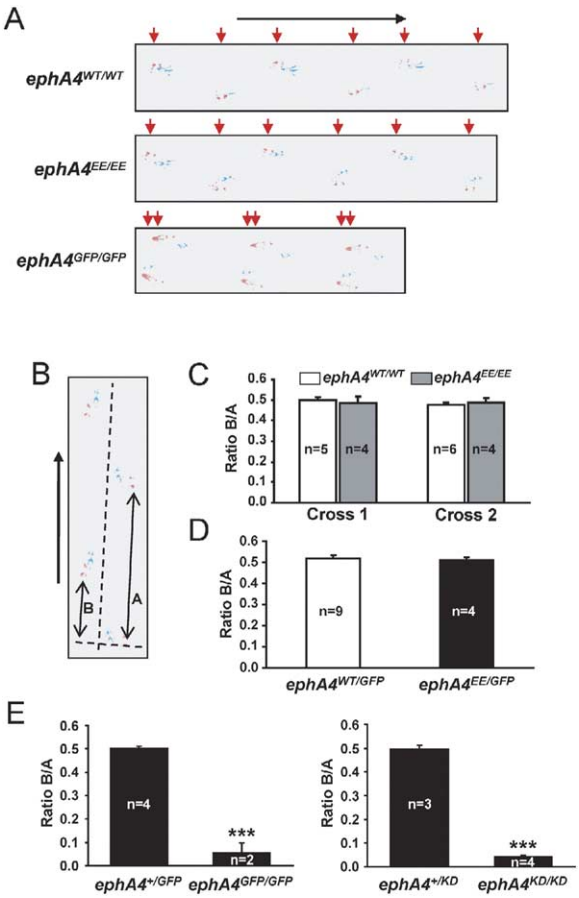

Figure 4. Gait Analysis of *ephA4*$^{EE/EE}$ Mutant Mice Reveals Normal Locomotion

(A) Mice were trained to travel a straight path to analyze their gait. Forepaws and hindpaws were stained with blue and red ink, respectively, to measure their placement during running. Vertical red arrows point to the position of the hindlimbs, and the horizontal black arrow on top indicates the direction of travel. Note the normal alternating profile in both the *ephA4*$^{WT/WT}$ and *ephA4*$^{EE/EE}$ mice. In contrast, the *ephA4*$^{GFP/GFP}$ footprints showed an almost simultaneous move of the hindpaws resulting in a hopping gait.

(B) Ratio between the distances covered by left and right paw (B) and the distance covered by the same paw (A) for quantification of the degree of parallel walking of the hindlimbs.

(C–E) Comparison of the B/A ratio between littermates of different experimental groups. (C) Comparison between homozygous *ephA4*$^{WT/WT}$ and *ephA4*$^{EE/EE}$ of two independent heterozygous crosses. Note that the *ephA4*$^{EE/EE}$ mice did not show any symptom of synchronicity and that they had a perfect alternating walking behavior even when an inactive copy of the *ephA4*^{GFP} receptor was present (D). (E) Homozygous mice expressing signaling-deficient EphA4 receptors (*ephA4*$^{GFP/GFP}$ and *ephA4*$^{KD/KD}$) showed a strong reduction in the B/A ratio, approaching the value 0.0. The numbers of mice used for these experiments are indicated. ***$p < 0.001$; Student's t test). Data in (C), (D), and (E) were expressed as the average ± SEM.

Dissociated *ephA4*$^{EE/EE}$ Neurons Display Normal Growth Cone Collapse Response

The results presented above indicated that, despite having deregulated kinase activity, the EphA4^{EE} mutant receptor was still able to normally regulate certain biological functions. The finding that EphA4-mediated events can occur at the right time and place during development even when the EphA4 kinase is constitutively active implies that when ephrins engage EphA4 during development a signaling mechanism must operate in addition to activation of the RTK to allow for normal development. To test this hypothesis, we used the in vitro growth cone collapse response of primary dissociated neurons derived from *ephA4* mutant mice (Figure 5A). Neurons from the embryonic part of the cortex that will give rise to the future motor cortex were chosen, because 85% of the cultured neurons expressed EphA4 (data not shown) and because neurons from this brain region project CST axons. Moreover, ephrinB3-induced growth cone collapse was strictly dependent on EphA4 signaling. As shown in Figure 5B, preclustered ephrinB3-Fc doubled the number of collapsed growth cones in cultures derived from heterozygous *ephA4*$^{GFP/+}$ neurons but was inert on homozygous *ephA4*$^{GFP/GFP}$ cultures. In contrast, ephrinA1-Fc was as effective on control and homozygous *ephA4*$^{GFP/GFP}$ cultures, suggesting that these neurons expressed additional EphA receptors. Notably, EphA4 kinase signaling was required, since ephrinB3-Fc failed to induce growth cone collapse of neurons expressing kinase-dead EphA4 (Figure 5C). Cultured neurons expressing kinase-active EphA4^{EE} receptors displayed the same rate of spontaneous growth cone collapse as control *ephA4*$^{WT/WT}$ neurons (Figure 5D), confirming the notion that activation of EphA4 kinase activity alone is not sufficient to trigger EphA4 signaling. Stimulation with preclustered ephrinB3-Fc induced the same collapse response in both neuron populations (Figure 5D), suggesting that ephrinB3 has an additional key function, possibly clustering of EphA4 that is independent of the induction of JM autophosphorylation.

Clustering of EphA4^{EE} Receptors Induces Growth Cone Collapse

Previous work using cultured cells had indicated that Eph signaling is sensitive to ligand oligomerization (Davis et al., 1994; Stein et al., 1998). However, it remained unclear whether different degrees of Eph clustering resulted in a concomitant increase in kinase activity. The kinase-active EphA4^{EE} receptor allowed us to uncouple clustering from regulation of kinase activity. We first asked if the *ephA4*^{EE} mutation changed the clustering behavior of EphA4. In a cell-cell assay using transfected HeLa cells, the EphA4^{EE} mutant receptor formed clusters upon contact with neighboring cells expressing ephrinB3, and EphA4^{EE} induced transendocytosis of ephrinB3 (Figure S4). More importantly, ligand-induced clustering properties of EphA4 in primary neurons were unchanged in the presence of EphA4^{EE}, including the number of axons with clusters, cluster density on the axons, and cluster size (Figure 6). Next, we asked if growth cone collapse of cortical neurons would be sensitive to ephrinB3 oligomerization. Indeed, we found that unclustered ephrinB3 was less potent than preclustered ephrinB3 in inducing growth cone collapse of neurons expressing kinase-active EphA4^{EE} receptor (Figure 7A). In contrast, the activity of ephrinA1, which appears to induce growth cone collapse largely independently of EphA4, was not influenced by preclustering (Figure 7A).

To directly address the role of receptor clustering in

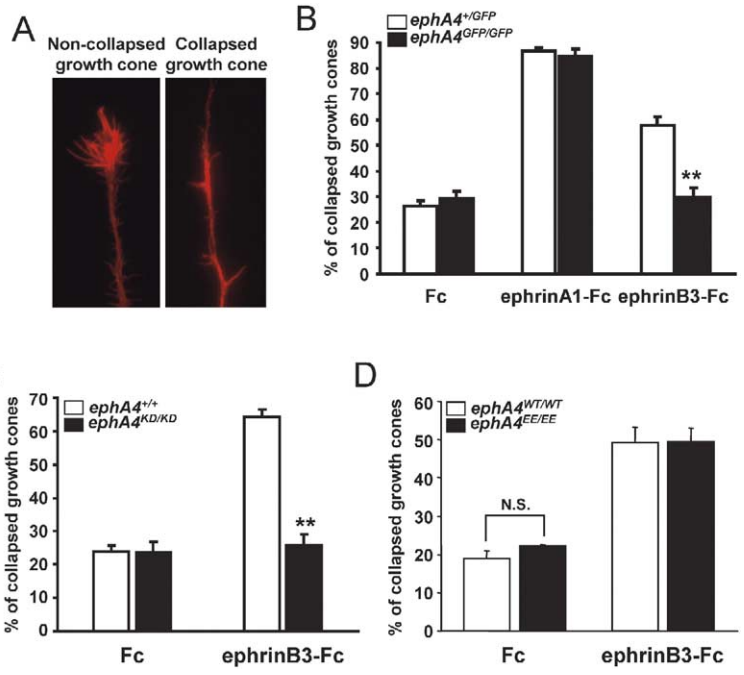

Figure 5. *EphA4*$^{EE/EE}$ Axons Display Normal In Vitro Growth Cone Collapse in Response to EphrinB3

(A) Representative examples of scored growth cones in phalloidin-stained cortical cultures treated with preclustered control Fc (left) or ephrinB3 (right). Note the reduced actin staining and the lack of filopodial extensions at the tip of the collapsed growth cone.

(B and C) Cultured cortical neurons from the indicated genotypes were stimulated for 30 min with 1 μg/ml of preclustered Fc, ephrinB3, or ephrinA1; fixed; stained with phalloidin; and scored for the percentage of collapsed growth cones. In the presence of the inactive EphA4^{GFP} (B) or EphA4^{KD} (C) receptor, ephrinB3 lost the ability to induce growth cone collapse, indicating that the ephrinB3-induced response was mainly mediated by EphA4. (**$p < 0.01$; Student's t test).

(D) Neurons from *ephA4*$^{EE/EE}$ or *ephA4*$^{WT/WT}$ mice were treated with preclustered Fc or ephrinB3 and processed as in (B) and (C). Control stimulated neurons from *ephA4*$^{EE/EE}$ mice displayed a similar fraction of collapsed growth cones as *ephA4*$^{WT/WT}$ neurons (N.S., nonsignificant). Similar collapse responses were induced by ephrinB3 in *ephA4*$^{EE/EE}$ neurons compared to *ephA4*$^{WT/WT}$ controls. Data were expressed as the average ± SEM.

regulating the biological function of EphA4, we raised an antibody against the globular domain (GD) of EphA4 (α-A4^{GD}) and used it to cluster EphA4 artificially, independently of ephrin, and to induce growth cone collapse. By Western blot analysis, the α-A4^{GD} antibody recognized specifically EphA4 in total cell lysates from embryonic brains (Figure S5A), and when added to the culture media of dissociated cortical neurons, it induced tyrosine phosphorylation of endogenous EphA4 comparable to exogenous ephrins (Figure S5B). In the growth cone collapse assay, the α-A4^{GD} antibody induced collapse of wild-type and heterozygous *ephA4*$^{GFP/+}$, but not of homozygous *ephA4*$^{GFP/GFP}$, neurons indicating that the antiserum specifically recognized EphA4 (Figure 7B). Importantly, the α-A4^{GD} antibody also induced growth cone collapse of homozygous *ephA4*$^{EE/EE}$ neurons, albeit somewhat less efficiently (Figure 7C), without a concomitant increase in the kinase activity of the EphA4^{EE} receptor (Figure 7D). Taken together, these results suggest that the biological readout of the EphA4^{EE} receptor is regulated by the degree of receptor clustering. They further suggest that the activation of distinct signaling cascades after receptor clustering does not require an increase in kinase activity.

EphA4^{EE} Receptor Induces Tyrosine Phosphorylation of the RhoGEF Ephexin1

At this point, we wanted to investigate the biochemical events that are triggered by ephrin stimulation downstream of the EphA4^{EE} receptor. Earlier work on Eph signaling had focused on SH2 domain-containing proteins that bind the two phosphorylated JM tyrosines (reviewed in Kullander and Klein, 2002). However, the EphA4^{EE} receptor is devoid of these two residues and yet is largely signaling competent, suggesting that under certain circumstances the primary role of these tyrosine residues is in the regulation of kinase activity (Wybenga-Groot et al., 2001; Zisch et al., 2000). More recently, small GTPases of the Rho family were shown to be required signaling effectors of Eph receptors (reviewed in Noren and Pasquale, 2004). One mediator of EphA4 signaling is ephexin1, a guanine exchange factor (GEF) protein for Rho GTPases that directly connects EphA receptors to cytoskeleton dynamics and growth cone mobility (Shamah et al., 2001). Recent work has shown that tyrosine phosphorylation of ephexin1 is required for ephrin-induced enhancement of its GEF activity toward Rho (Sahin et al., 2005). We therefore tested ephexin1 as a candidate, whose activity (phosphorylation) might be triggered by Eph clustering independently of Eph kinase regulation. Different EphA4 cDNAs were overexpressed in HeLa cells together with a FLAG-tagged version of ephexin1, which after immunoprecipitation from cell lysates was analyzed by Western blotting using an antibody against phosphorylated ephexin (P-ephexin). As shown in Figure 8A, ephexin1 only became tyrosine phosphorylated when cotransfected with EphA4^{WT} or EphA4^{EE} receptors, but not with the signaling-deficient mutants EphA4^{KD} or EphA4^{GFP} (data not shown). The phosphorylation signal recognized by the antibody was specific, since it could not be detected when a mutant form of ephexin1 was used in which Y87 was replaced by phenylalanine (data not shown).

We next asked if ephexin1 phosphorylation could be induced by ephrin stimulation in our cortical neuron cultures and if this event was dependent on EphA4 signaling. Both preclustered ephrinA1-Fc and ephrinB3-Fc

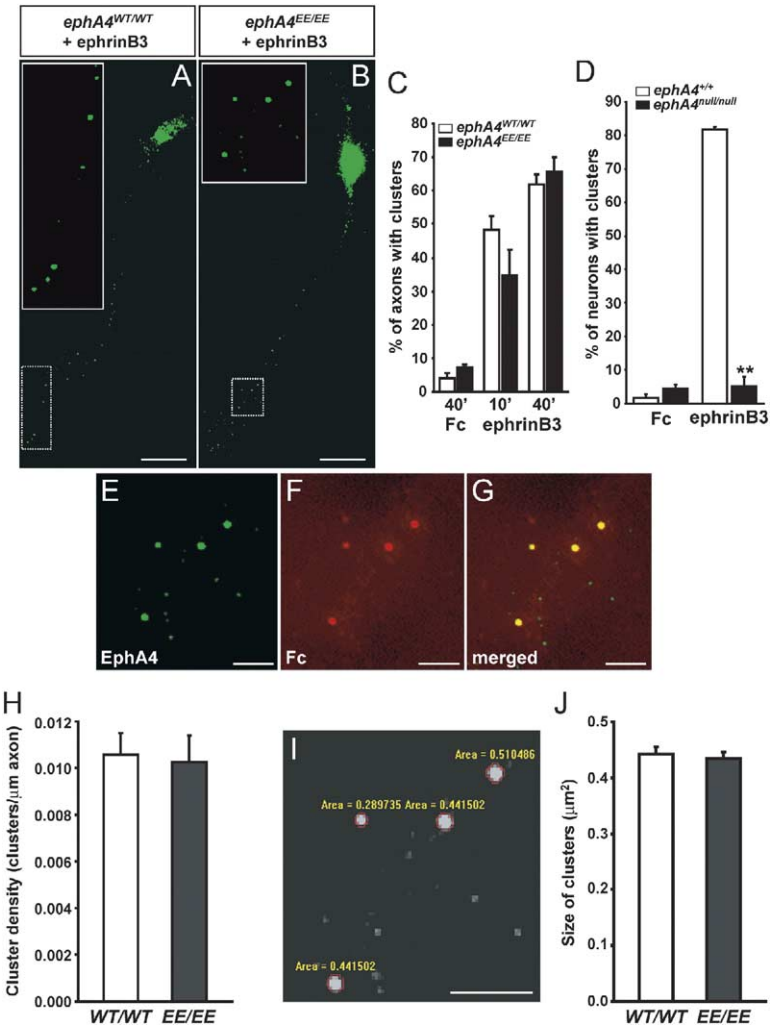

Figure 6. Analysis of the Clustering Properties of the EphA4^{EE} Receptor

Neurons were incubated for 2DIV and stimulated for the indicated time points with 1–3 μg/ml of preclustered Fc or ephrinB3-Fc. After fixation, the neurons were permeabilized and stained with anti-EphA4 (S20 from Santa Cruz) and anti-Fc. (A and B) Representative ephrinB3-stimulated neurons of the indicated genotypes stained with anti-EphA4. Stippled boxes in (A) and (B) indicate those areas that are enlarged. Scale bars, 15 μm. (C) Quantification of stimulated neurons (in percent of total neurons) with at least one bright EphA4 cluster in the main axon. Stimulation was done for 10 and 40 min. (D) Specificity of anti-EphA4 staining. The bright clusters recognized by the S20 antibody in ephrinB3-stimulated wild-type neurons are not present in the *ephA4$^{null/null}$* neurons, indicating that the antibody is highly specific for EphA4 (**$p < 0.01$; Student's t test). (E–G) Representative images of the clusters recognized by anti-EphA4 (S20) (E) and by anti-Fc antibodies ([F]; merged in [G]). Scale bars, 3 μm. (H) Quantification of the density of anti-EphA4 and anti-Fc-positive clusters per μm axon. The graph shows the average cluster density ± SEM of 23 (*ephA4$^{WT/WT}$*) and 29 neurons (*ephA4$^{EE/EE}$*). (I) Representative image of an axon after anti-EphA4 staining (same as in [E]) showing the measurement of cluster area (=cluster size) using the Metamorph software. The indicated values were converted from pixel^2 into μm^2. Scale bar, 3 μm. (J) Comparison of cluster size (±SEM) between *ephA4$^{WT/WT}$* (n = 30) and *ephA4$^{EE/EE}$* neurons (n = 32). For each neuron, a mean cluster size was obtained by pooling the data from 5 to 22 double-positive clusters. Data were expressed as the average ± SEM.

induced the phosphorylation of ephexin1 compared to control Fc (Figure 8B). However, only the phosphorylation of ephexin1 by ephrinB3-Fc was EphA4 dependent (Figure 8B), which correlated with the growth cone collapse responses. Importantly, ephexin1 phosphorylation was also induced by ephrinB3 stimulation of kinase-active EphA4^{EE} receptor, and the degree of ephexin1 phosphorylation was comparable to wild-type EphA4 (Figure 8C). These results demonstrate that the kinase-active EphA4^{EE} receptor mediates phosphorylation of ephexin1 and that this event is controlled by clustering of EphA4^{EE} by ephrinB3. Therefore, ephexin1 phosphorylation is an event that correlates with the ability of EphA4^{EE} to mediate axonal growth cone collapse.

Discussion

Here, we have shown that a constitutively active EphA4 receptor mediates several of the in vivo functions that require EphA4 forward signaling. These results were rather unexpected, since based on previous work with other RTKs, we expected the EphA4^{EE} receptor to behave abnormally. We hypothesized that a navigating growth cone with a constitutively active Eph receptor would undergo spontaneous collapse in the absence of ephrin engagement. Consequently, the formation of axon tracts expressing EphA4 would have been defective or severely delayed. We further reasoned that a constitutively active EphA4 receptor may trigger increased endocytosis and intracellular trafficking which would reduce the concentration of EphA4 in the plasma membrane and the sensitivity toward ephrins. In this case, the phenotype would have been similar to a loss-of-function allele. Unexpectedly, EphA4^{EE} mediated normal development under several circumstances, suggesting that EphA4^{EE} engaged ephrins normally whenever the growth cone contacted an ephrin-expressing cell population. The fact that EphA4^{EE} is fully activated with respect to its kinase activity before ephrin engagement suggests that the ephrins trigger events in addition to activating the kinase. Our in vitro growth cone collapse assays suggest that ephrins activate EphA4 signaling by higher-order clustering. Clustering in turn induces the phosphorylation of ephexin1, a modification that leads to activation of its exchange

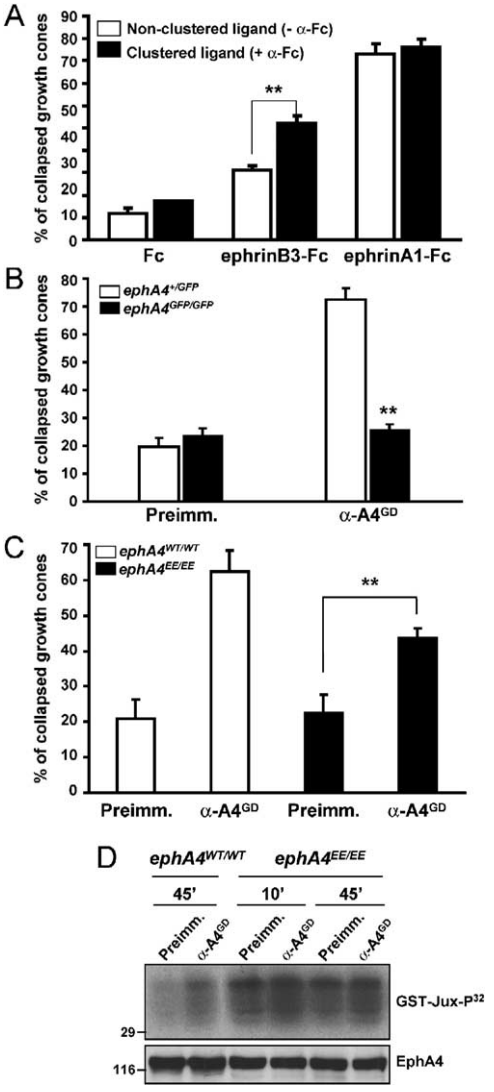

Figure 7. Receptor Clustering Regulates the Growth Cone Collapse Response of *ephA4*$^{EE/EE}$ Neurons

(A) Cultured cortical neurons from *ephA4*$^{EE/EE}$ mutant mice were stimulated for 30 min with 1 μg/ml of nonclustered or preclustered Fc, ephrinB3, or ephrinA1; fixed; stained with phalloidin; and scored for the percentage of collapsed growth cones. Nonclustered ephrinB3 ligand was less effective than preclustered ephrinB3 in inducing growth cone collapse. (**$p < 0.01$; Student's t test). (B and C) Neurons from the indicated genotypes were treated for 30 min with the antibody directed against the globular domain of EphA4 (α-A4^{GD} antibody; 30 μl of crude serum/ml of media) and processed as in (A). (B) The α-A4^{GD}-induced growth cone collapse is mainly mediated by EphA4, since its ability to induce collapse was dependent on the presence of a signaling-competent EphA4 receptor. (C) Clustering of EphA4 by α-A4^{GD} antibodies induced growth cone collapse even in the presence of the kinase-active EphA4^{EE} receptor (**$p < 0.01$; Student's t test). (D) EphA4 kinase activity toward the exogenous substrate GST-JM in immunoprecipitates from cortical neurons derived from control *ephA4*$^{WT/WT}$ or *ephA4*$^{EE/EE}$ neurons. While clustering of EphA4^{WT} with α-A4^{GD} antibodies increased the kinase activity of the receptor compared to preimmune serum, clustering of EphA4^{EE} did not. Data were expressed as the average ± SEM.

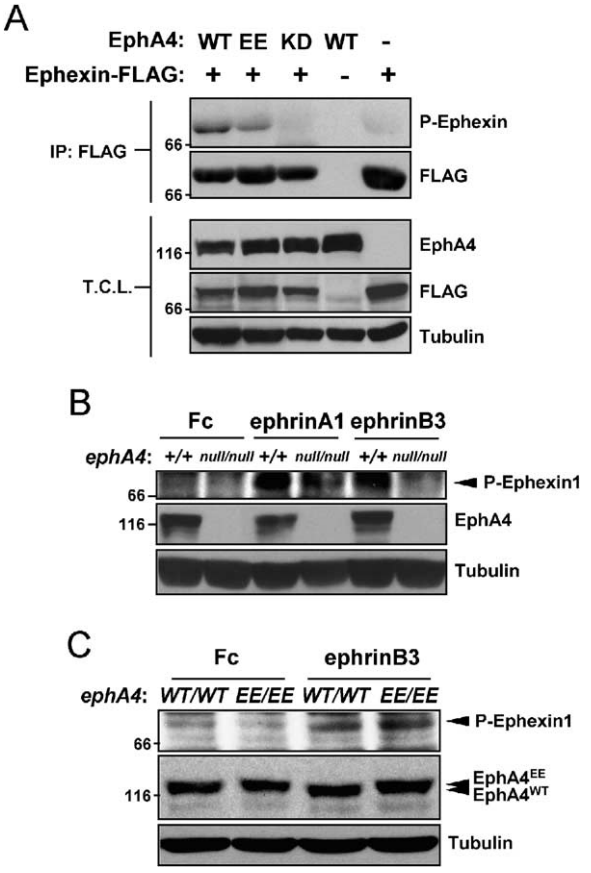

Figure 8. The EphA4^{EE} Receptor Retains the Ability to Phosphorylate Ephexin1 upon Ligand Stimulation

(A) HeLa cells were cotransfected with different versions of EphA4 and FLAG-tagged ephexin1 as indicated, and cell lysates were subjected to FLAG immunoprecipitation. Samples were then analyzed by Western blotting using an anti-P-ephexin1 antibody and then reprobed with an anti-FLAG antibody for loading control. EphA4^{WT} and EphA4^{EE} but not the inactive EphA4^{KD} receptor were able to induce ephexin1 phosphorylation (top panel). The lower three panels show the expression levels of the indicated proteins in the same total cell lysates (T.C.L.) used for immunoprecipitation (FLAG for ephexin1).

(B) Cultured cortical neurons from wild-type (+/+) or *ephA4*$^{null/null}$ mice (–/–) were stimulated as indicated with 2 μg/ml of Fc (10 min), ephrinA1 (10 min), or ephrinB3 (30 min), and total cell lysates were subjected to Western blot analysis against anti-P-ephexin1. The P-ephexin1 antibody gave a complex pattern of bands (data not shown). A band of ~70 kDa was specifically phosphorylated after ephrin stimulation and disappeared in lysates derived from ephexin1 knockout mice (Sahin et al., 2005). Both ephrinA1 and ephrinB3 induced phosphorylation of the 70 kDa ephexin1 band in +/+ neurons (arrow). In ephrinB3-stimulated *ephA4*$^{null/null}$ neurons, ephexin1 phosphorylation was not induced (lane furthest to the right). EphrinA1 was still able to partially induce ephexin1 phosphorylation in *ephA4*$^{null/null}$ neurons. Middle and lower panels show expression controls for EphA4 and tubulin, respectively.

(C) Cultured cortical neurons from *ephA4*$^{WT/WT}$ or *ephA4*$^{EE/EE}$ mice were stimulated with Fc or ephrinB3 (as in [B]) to induce ephexin1 phosphorylation specifically through EphA4. The degree of ephexin1 phosphorylation in *ephA4*$^{EE/EE}$ neurons was comparable to that in *ephA4*$^{WT/WT}$ neurons.

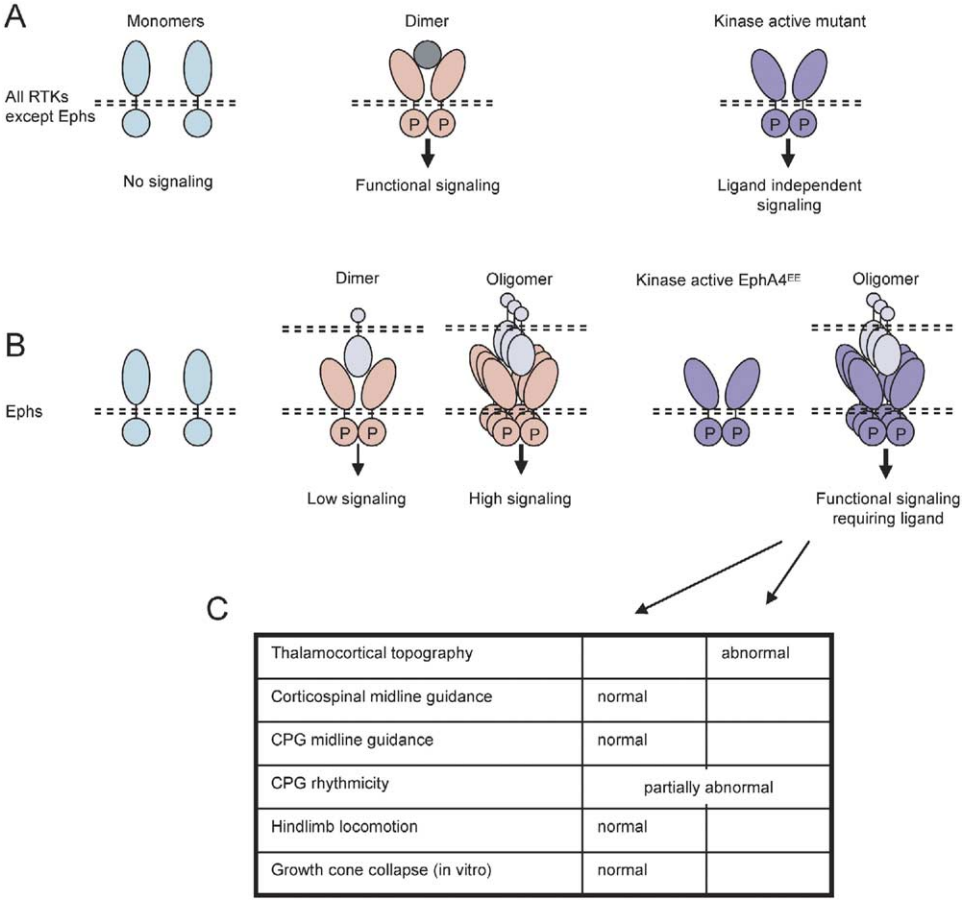

C

Thalamocortical topography		abnormal
Corticospinal midline guidance	normal	
CPG midline guidance	normal	
CPG rhythmicity	partially abnormal	
Hindlimb locomotion	normal	
Growth cone collapse (in vitro)	normal	

Figure 9. Comparative Model of RTK and Eph Activation

(A) Inactive RTK monomers (light blue, left panel) are in equilibrium with receptor dimers (data not shown). Ligand binding stabilizes dimer formation in a conformation compatible with trans-autophosphorylation and stimulation of kinase activity (pink, middle panel) (adapted with permission from Schlessinger, 2000). This process is sufficient for functional signaling. Mutations that generate kinase-active mutant RTKs result in ligand-independent signaling and gain-of-function phenotypes (purple, right panel).

(B) Inactive Eph monomers (light blue, left panel) are dimerized by binding ephrins and are trans-autophosphorylated similar to other RTKs. However, some biological functions require organization into an active oligomer by higher-order clustering of the Eph-ephrin complex. The EphA4^{EE} mutant carrying a constitutively active kinase is regulated normally by ephrin clustering and mediates most in vivo functions (purple, right panel).

(C) Summary of EphA4-dependent in vivo functions analyzed in *ephA4^{EE}* mutant mice.

activity toward Rho GTPase. We propose a model in which the activation of Eph RTKs follows a multistep process of induced kinase activity and higher-order clustering that is different from the activation mechanism of other RTK subfamilies.

RTKs are thought to exist in equilibrium between inactive monomers and inactive or active dimers. According to this model, ligand binding stabilizes active dimer formation and activation of the receptor's intrinsic kinase activity. Active dimers undergo rapid autophosphorylation, thereby creating docking sites for signaling proteins (reviewed in Schlessinger, 2000) (Figure 9A). The biological activity of RTKs strictly correlates with the degree of enzymatic activation. Mutations that generate kinase-active mutant RTKs result in ligand-independent signaling and gain-of-function phenotypes, such as hyperproliferation or cell transformation. In rodents, kinase-active RTK mutants cause developmental syndromes or predisposition to cancer (Holland et al., 1998; Sommer et al., 2003). The JM region of RTKs appears to be a particularly sensitive region for transforming mutations. In several RTKs, the JM domain autoinhibits the kinase domain by intramolecular interaction with the N-terminal lobe of the kinase (Herbst and Burden, 2000; Wybenga-Groot et al., 2001). Activating mutations in the JM domain have been frequently reported (Gille et al., 2000; Irusta and DiMaio, 1998).

Eph signaling appears to be controlled in a different manner (Figure 9B). Our results with EphA4 suggest that the first step of ligand-mediated autophosphorylation occurs in a similar fashion to other RTKs, but that this step is not sufficient to generate a functional readout. Mutation of the EphA4 JM region results in a constitutively active receptor, whose basal kinase activity is comparable to or even higher than that of ligand-

stimulated wild-type receptor and whose kinase activity can only be minimally stimulated (if at all) by ligand binding. Yet, its signaling output can still be regulated by ligand under certain circumstances. Therefore, Eph signaling requires an additional level of regulation, which most likely is the formation of higher-order clusters and the activation of distinct signaling events. In previous work using in vitro cultures of primary endothelial and transfected cell lines, soluble forms of ephrinBs had been shown to stimulate Eph signaling when aggregated into clusters suggesting that Ephs were sensitive to the oligomeric state of ephrins (Davis et al., 1994; Stein et al., 1998). From this work, it remained unclear whether the degree of Eph clustering also regulated the level of kinase activity. In other words, the larger the Eph clusters were, the higher Eph kinase activity would be. In an alternative scenario, Eph kinase activity was already fully activated by dimerization, and higher-order clustering would not lead to a further increase in Eph kinase activity, but rather to the recruitment of a new set of cytoplasmic effectors. Our results with constitutively active EphA4^{EE} support the latter scenario. Ephrin-induced clustering of EphA4^{EE} can produce a normal cellular response despite the fact that its kinase activity cannot be further increased.

The phosphorylation of ephexin1 appears to be one of the key steps in repulsive guidance mediated by EphAs. Ephexin1 had previously been shown to interact with the cytoplasmic domain of EphA4 and to modulate ephrin-induced RhoA activation, Cdc42 and Rac1 inhibition, and cell morphology changes (Shamah et al., 2001). Using neurons derived from *ephexin1* knockouts, ephexin1 was shown to be required for ephrin-induced growth cone collapse. Mechanistically, EphA4 signaling leads to tyrosine phosphorylation of ephexin1, a modification that enhances ephexin1's substrate preference for RhoA, while not altering its activity toward Rac1 and Cdc42, changing the balance of GTPase activities. Importantly, ephexin1 phosphorylation is required for growth cone collapse (Sahin et al., 2005). Recent work suggests that ephexin1 is a substrate of Src family kinases (SFKs) downstream of EphA4-mediated retinal axon guidance (Knoll and Drescher, 2004; Sahin et al., 2005). Our results have shown that ephexin1 phosphorylation is controlled by ephrin-Eph clustering. This modification is also mediated by kinase-active EphA4^{EE}, suggesting that this is a process that happens largely independently of the regulation of EphA4 kinase activity. We suggest that ephexin1 is recruited into higher-order clusters of EphA4 along with SFKs and possibly other effector proteins. This leads to the activation of Src kinase activity and subsequent ephexin1 phosphorylation by Src.

Among the diverse in vivo functions of EphA4, thalamocortical projections were not rescued by kinase-active ephA4^{EE}. One of the possible explanations is that thalamocortical projections are controlled by ephrinA5, whereas midline guidance of CST and CPG axons is provided by ephrinB3. It is possible that the functional requirement for regulated kinase activity differs depending on whether the receptor is activated by ephrinA or ephrinB ligands. Secondly, the intrinsic response of thalamic neurons to EphA4 signaling may be different from that of corticospinal or spinal cord interneurons. The JM tyrosine residues that were mutated in ephA4^{EE}, besides controlling the kinase activity of the receptor, have been shown to bind SH2 domain-containing effector proteins (reviewed in Kullander and Klein, 2002). It is conceivable that thalamic neurons require an EphA4 effector that binds to phosphorylated JM tyrosine residues.

A final possibility for the phenotype in thalamocortical projections may be the fact that they are topographic and EphA4 has to respond to a smooth gradient of ligand, whereas midline guidance is achieved by a step gradient of ligand. The ability to generate a graded response to ephrins likely requires a particularly tight regulation of Eph activation (Hansen et al., 2004), including its phosphorylation state: in this context the dynamic range of sensitivity of EphA4 to ephrin gradients could be impaired in *ephA4$^{EE/EE}$* mutants, hence leading to the topographic errors observed in vivo in the thalamocortical system. It would be interesting to set up in vitro assays challenging the EphA4^{EE} receptor with either smooth or step gradients of the same ligand to investigate whether the regulation of kinase activity is more critical when the growth cone has to sense an ephrin gradient. In this respect, it is interesting to note that the physiology of the CPG was not completely normal in the *ephA4$^{EE/EE}$* mutants. In the normal spinal cord, EphA4 signaling is required for CPG neurons projecting ipsilaterally to an unknown target and responding to so far uncharacterized ephrins. We observed a certain degree of drifting of firing patterns between L2 and L5 and aberrant synchrony at lumbar level 5 in the *ephA4$^{EE/EE}$* mutants, which was not observed in controls. It is tempting to speculate that the EphA4-dependent ipsilateral projections are topographically organized and that they follow similar constraints as the thalamocortical projections. If this were true, then EphA4 would have two distinct functions in the spinal CPG: first, to prevent aberrant midline crossing (rescued by EphA4^{EE}) and, second, to provide ipsilateral topography (partially rescued by EphA4^{EE}).

Experimental Procedures

Generation of *ephA4^{EE}* Mutant Mice

Mutant *ephA4^{EE}* mice were generated using the same replacement-type targeting strategy previously described (Kullander et al., 2001b). The mutant *ephA4^{EE}* allele encoded EphA4 with the two JM tyrosine residues Y596 and Y602 replaced by glutamic acids. The loxP-flanked neo cassette was removed in vivo by crossbreeding to a Cre recombinase expressing transgenic mouse strain, and all mutant phenotypes were analyzed in comparable mixed 129/Svev × C57Bl/6 backgrounds.

Tracing Experiments and Tissue Processing

Retrograde tracing of the VB nucleus of the thalamus was performed as previously described (Dufour et al., 2003). Tracing of the corticospinal tract with the anterograde tracer biotin dextrane amine was done as previously described (Kullander et al., 2001b) (see also Supplemental Experimental Procedures).

Gait Analysis

Gait analysis was conducted in littermate animals as previously described (Kullander et al., 2001a). In order to minimize the differences in sex, weight, and speed within a group of mice, we have obtained a parameter from the ratio depicted in Figure 4B for each step. For each mouse, an average value was obtained from 10 to 20 steps, and for each group two to nine animals were considered.

Data were analyzed by Student's t test and expressed as the average ± SEM.

Electrophysiology and Circular Statistics

Isolated spinal cords obtained from neonates (P0–P3) were placed in a recording chamber as previously described (Kjaerulff and Kiehn, 1996). Fictive locomotion was induced by perfusion with NMDA (3–8 μM) and serotonin creatine sulfate (5-HT; 3–15 μM) and registered by recordings from the left ("l" in Figure 3) and right ("r" in Figure 3) L2 and L5 roots (see also Supplemental Experimental Procedures).

Primary Cell Culture and Growth Cone Collapse Assay

Neuronal cultures were established as described (Kullander et al., 2001a) and stimulated with 1–2 μg/ml of the indicated ephrin-Fc ectodomain fusion proteins (R&D Systems, Minneapolis, MN) or with Fc only as a control (Jackson Immuno Research, West Grove, PA). Fc or ephrin-Fc fusion proteins were preclustered with an anti-Fc antibody (Jackson ImmunoResearch) for 1 hr at room temperature in a 5:1 molar ratio. Stimulation with the α-A4^{GD} antibody (see below) was carried out adding 30 μl of the crude antiserum per ml of media. The antibody was previously incubated with an anti-rabbit antibody (Jackson ImmunoResearch) in a 10:1 volume ratio. Growth cone collapse assays were performed as previously described (Kullander et al., 2001a) (see also Supplemental Experimental Procedures).

Cell Transfection and Cell-Cell Stimulation Assay

HeLa or HEK293 cells transiently transfected using standard calcium phosphate/DNA precipitation procedure were used in cell-cell stimulation assays as previously described (Zimmer et al., 2003).

In Vitro Kinase Assay

In vitro kinase assays were done as described (Kullander et al., 2001b) using 2–4 μl of the anti-EphA4 antiserum (Becker et al., 1995) (more information in Supplemental Experimental Procedures). Glutathione S-transferase (GST)-JM fusion protein was generated by subcloning a PCR product including the JM tyrosines of the mouse EphA4 (sequence RSKY . . . CVAI) in frame with the GST into the bacteria expression vector pGEX-2T. Protein was produced in BL21 bacteria (Stratagene, Torrey Pines Road, CA) and purified using a glutathione matrix column (Amersham Biosciences).

Supplemental Data

The Supplemental Data include Supplemental Experimental Procedures and five figures and can be found with this article online at http://www.neuron.org/cgi/content/full/47/4/515/DC1/.

Acknowledgments

We thank K. Vintersten (EMBL) for help with generating the *ephA4*^{EE} mutant mice; M. Schwanders (MPIN mouse facility) for mouse husbandry; P. Charnay for reagents; R. Sanchez, F. Helmbacher, and J. Koehler for intellectual input throughout this work; and T. Mäkinen and G.A. Wilkinson for critically reading the manuscript. J.E. is a Marie Curie/EMBO fellow. This work was in part funded by grants from the Deutsche Forschungsgemeinschaft and by the Max-Planck Society (to R.K.). We thank the Norwegian Medical Research Council (EMBIO Ph.D. stipend to U.V.N.) and the Swedish Research Council, HFSP, and NIH for grant support to O.K. We acknowledge grants from Belgian FNRS, FMRE, and IUAP Programmes (to P.V.). P.V. is a Research Associate of the FNRS, and A.D. is a FRIA Fellow.

Received: December 16, 2004
Revised: May 13, 2005
Accepted: June 26, 2005
Published: August 17, 2005

References

Bardelli, A., Longati, P., Gramaglia, D., Basilico, C., Tamagnone, L., Giordano, S., Ballinari, D., Michieli, P., and Comoglio, P.M. (1998). Uncoupling signal transducers from oncogenic MET mutants abrogates cell transformation and inhibits invasive growth. Proc. Natl. Acad. Sci. USA *95*, 14379–14383.

Becker, N., Gilardi-Hebenstreit, P., Seitanidou, T., Wilkinson, D., and Charnay, P. (1995). Characterisation of the Sek-1 receptor tyrosine kinase. FEBS Lett. *368*, 353–357.

Butt, S.J., and Kiehn, O. (2003). Functional identification of interneurons responsible for left-right coordination of hindlimbs in mammals. Neuron *38*, 953–963.

Chen, L.I., Webster, M.K., Meyer, A.N., and Donoghue, D.J. (1997). Transmembrane domain sequence requirements for activation of the p185c-neu receptor tyrosine kinase. J. Cell Biol. *137*, 619–631.

Chiarugi, P., Taddei, M.L., Schiavone, N., Papucci, L., Giannoni, E., Fiaschi, T., Capaccioli, S., Raugei, G., and Ramponi, G. (2004). LMW-PTP is a positive regulator of tumor onset and growth. Oncogene *23*, 3905–3914.

Cowan, C.A., Yokoyama, N., Saxena, A., Chumley, M.J., Silvany, R.E., Baker, L.A., Srivastava, D., and Henkemeyer, M. (2004). Ephrin-B2 reverse signaling is required for axon pathfinding and cardiac valve formation but not early vascular development. Dev. Biol. *271*, 263–271.

Cowley, K.C., and Schmidt, B.J. (1997). Regional distribution of the locomotor pattern-generating network in the neonatal rat spinal cord. J. Neurophysiol. *77*, 247–259.

Davis, S., Gale, N.W., Aldrich, T.H., Maisonpierre, P.C., Lhotak, V., Pawson, T., Goldfarb, M., and Yancopoulos, G.D. (1994). Ligands for EPH-related receptor tyrosine kinases that require membrane attachment or clustering for activity. Science *266*, 816–819.

Dufour, A., Seibt, J., Passante, L., Depaepe, V., Ciossek, T., Frisen, J., Kullander, K., Flanagan, J.G., Polleux, F., and Vanderhaeghen, P. (2003). Area specificity and topography of thalamocortical projections are controlled by ephrin/Eph genes. Neuron *39*, 453–465.

Gerlai, R., Shinsky, N., Shih, A., Williams, P., Winer, J., Armanini, M., Cairns, B., Winslow, J., Gao, W., and Phillips, H.S. (1999). Regulation of learning by EphA receptors: a protein targeting study. J. Neurosci. *19*, 9538–9549.

Gille, H., Kowalski, J., Yu, L., Chen, H., Pisabarro, M.T., Davis-Smyth, T., and Ferrara, N. (2000). A repressor sequence in the juxtamembrane domain of Flt-1 (VEGFR-1) constitutively inhibits vascular endothelial growth factor-dependent phosphatidylinositol 3′-kinase activation and endothelial cell migration. EMBO J. *19*, 4064–4073.

Grunwald, I.C., Korte, M., Adelmann, G., Plueck, A., Kullander, K., Adams, R.H., Frotscher, M., Bonhoeffer, T., and Klein, R. (2004). Hippocampal plasticity requires postsynaptic ephrinBs. Nat. Neurosci. *7*, 33–40.

Hansen, M.J., Dallal, G.E., and Flanagan, J.G. (2004). Retinal axon response to ephrin-As shows a graded, concentration-dependent transition from growth promotion to inhibition. Neuron *42*, 717–730.

Herbst, R., and Burden, S.J. (2000). The juxtamembrane region of MuSK has a critical role in agrin-mediated signaling. EMBO J. *19*, 67–77.

Himanen, J.P., Chumley, M.J., Lackmann, M., Li, C., Barton, W.A., Jeffrey, P.D., Vearing, C., Geleick, D., Feldheim, D.A., Boyd, A.W., et al. (2004). Repelling class discrimination: ephrin-A5 binds to and activates EphB2 receptor signaling. Nat. Neurosci. *7*, 501–509.

Holland, E.C., Hively, W.P., DePinho, R.A., and Varmus, H.E. (1998). A constitutively active epidermal growth factor receptor cooperates with disruption of G1 cell-cycle arrest pathways to induce glioma-like lesions in mice. Genes Dev. *12*, 3675–3685.

Irusta, P.M., and DiMaio, D. (1998). A single amino acid substitution in a WW-like domain of diverse members of the PDGF receptor subfamily of tyrosine kinases causes constitutive receptor activation. EMBO J. *17*, 6912–6923.

Kaprielian, Z., Runko, E., and Imondi, R. (2001). Axon guidance at the midline choice point. Dev. Dyn. *221*, 154–181.

Kiehn, O., and Kjaerulff, O. (1998). Distribution of central pattern generators for rhythmic motor outputs in the spinal cord of limbed vertebrates. Ann. N Y Acad. Sci. *860*, 110–129.

Kiehn, O., and Kullander, K. (2004). Central pattern generators deciphered by molecular genetics. Neuron *41*, 317–321.

Kjaerulff, O., and Kiehn, O. (1996). Distribution of networks generating and coordinating locomotor activity in the neonatal rat spinal cord in vitro: a lesion study. J. Neurosci. *16*, 5777–5794.

Knoll, B., and Drescher, U. (2004). Src family kinases are involved in EphA receptor-mediated retinal axon guidance. J. Neurosci. *24*, 6248–6257.

Kremer, E., and Lev-Tov, A. (1997). Localization of the spinal network associated with generation of hindlimb locomotion in the neonatal rat and organization of its transverse coupling system. J. Neurophysiol. *77*, 1155–1170.

Kullander, K., and Klein, R. (2002). Mechanisms and functions of Eph and ephrin signalling. Nat. Rev. Mol. Cell Biol. *3*, 475–486.

Kullander, K., Croll, S.D., Zimmer, M., Pan, L., McClain, J., Hughes, V., Zabski, S., DeChiara, T.M., Klein, R., Yancopoulos, G.D., and Gale, N.W. (2001a). Ephrin-B3 is the midline barrier that prevents corticospinal tract axons from recrossing, allowing for unilateral motor control. Genes Dev. *15*, 877–888.

Kullander, K., Mather, N.K., Diella, F., Dottori, M., Boyd, A.W., and Klein, R. (2001b). Kinase-dependent and kinase-independent functions of EphA4 receptors in major axon tract formation in vivo. Neuron *29*, 73–84.

Kullander, K., Butt, S.J., Lebret, J.M., Lundfald, L., Restrepo, C.E., Rydstrom, A., Klein, R., and Kiehn, O. (2003). Role of EphA4 and EphrinB3 in local neuronal circuits that control walking. Science *299*, 1889–1892.

Noren, N.K., and Pasquale, E.B. (2004). Eph receptor-ephrin bidirectional signals that target Ras and Rho proteins. Cell. Signal. *16*, 655–666.

Palmer, A., and Klein, R. (2003). Multiple roles of ephrins in morphogenesis, neuronal networking, and brain function. Genes Dev. *17*, 1429–1450.

Pasini, A., Geneste, O., Legrand, P., Schlumberger, M., Rossel, M., Fournier, L., Rudkin, B.B., Schuffenecker, I., Lenoir, G.M., and Billaud, M. (1997). Oncogenic activation of RET by two distinct FMTC mutations affecting the tyrosine kinase domain. Oncogene *15*, 393–402.

Sahin, M., Greer, P.L., Lin, M.Z., Poucher, H., Eberhart, J., Schmidt, S., Wright, T.M., Shamah, S.M., O'Connell, S., Cowan, C.W., et al. (2005). Eph-dependent tyrosine phosphorylation of ephexin1 modulates growth cone collapse. Neuron *46*, 191–204.

Schlessinger, J. (2000). Cell signaling by receptor tyrosine kinases. Cell *103*, 211–225.

Shamah, S.M., Lin, M.Z., Goldberg, J.L., Estrach, S., Sahin, M., Hu, L., Bazalakova, M., Neve, R.L., Corfas, G., Debant, A., and Greenberg, M.E. (2001). EphA receptors regulate growth cone dynamics through the novel guanine nucleotide exchange factor ephexin. Cell *105*, 233–244.

Sommer, G., Agosti, V., Ehlers, I., Rossi, F., Corbacioglu, S., Farkas, J., Moore, M., Manova, K., Antonescu, C.R., and Besmer, P. (2003). Gastrointestinal stromal tumors in a mouse model by targeted mutation of the Kit receptor tyrosine kinase. Proc. Natl. Acad. Sci. USA *100*, 6706–6711.

Stein, E., Lane, A.A., Cerretti, D.P., Schoecklmann, H.O., Schroff, A.D., Van Etten, R.L., and Daniel, T.O. (1998). Eph receptors discriminate specific ligand oligomers to determine alternative signaling complexes, attachment, and assembly responses. Genes Dev. *12*, 667–678.

Vanderhaeghen, P., and Polleux, F. (2004). Developmental mechanisms patterning thalamocortical projections: intrinsic, extrinsic and in between. Trends Neurosci. *27*, 384–391.

Wimmer-Kleikamp, S.H., Janes, P.W., Squire, A., Bastiaens, P.I., and Lackmann, M. (2004). Recruitment of Eph receptors into signaling clusters does not require ephrin contact. J. Cell Biol. *164*, 661–666.

Wybenga-Groot, L.E., Baskin, B., Ong, S.H., Tong, J., Pawson, T., and Sicheri, F. (2001). Structural basis for autoinhibition of the Ephb2 receptor tyrosine kinase by the unphosphorylated juxtamembrane region. Cell *106*, 745–757.

Yokoyama, N., Romero, M.I., Cowan, C.A., Galvan, P., Helmbacher, F., Charnay, P., Parada, L.F., and Henkemeyer, M. (2001). Forward signaling mediated by ephrin-B3 prevents contralateral corticospinal axons from recrossing the spinal cord midline. Neuron *29*, 85–97.

Zimmer, M., Palmer, A., Kohler, J., and Klein, R. (2003). EphB-ephrinB bi-directional endocytosis terminates adhesion allowing contact mediated repulsion. Nat. Cell Biol. *5*, 869–878.

Zisch, A.H., Pazzagli, C., Freeman, A.L., Schneller, M., Hadman, M., Smith, J.W., Ruoslahti, E., and Pasquale, E.B. (2000). Replacing two conserved tyrosines of the EphB2 receptor with glutamic acid prevents binding of SH2 domains without abrogating kinase activity and biological responses. Oncogene *19*, 177–187.